



An Investigation of the Physicochemical and Thermal Characteristics of Consciousness Energy Healing Treated L-Cysteine



Gopal Nayak¹, Mahendra Kumar Trivedi¹, Alice Branton¹, Dahryn Trivedi¹ and Snehasis Jana^{2*}

¹Trivedi Global, Inc., USA

²Trivedi Science Research Laboratory Pvt Ltd, Bhopal, India

Submission: September 14, 2018; **Published:** November 30, 2018

***Corresponding author:** Snehasis Jana, Trivedi Science Research Laboratory Pvt. Ltd., Bhopal, India

Abstract

L-cysteine is an essential amino acid that helps in improving the overall health status of humans. The objective of the study was to determine the impact on the physicochemical and thermal properties of L-cysteine after the Trivedi Effect[®]-Consciousness Energy Healing Treatment using modern analytical techniques. The control sample was kept without any treatment, while the Biofield Treatment was given to the treated sample remotely by a renowned Biofield Energy Healer, Gopal Nayak. The particle size values were significantly reduced by 11.96%(d₁₀), 9.01%(d₅₀), 4.92%(d₉₀), and 7.66% [D (4, 3)], thus, the specific surface area was significantly increased by 14.28% of the treated L-cysteine compared to the control sample. The peak intensities and crystallite sizes were altered ranging from -86.73% to 456.65% and -4.91% to 451.22% respectively, however, the average crystallite size was significantly increased by 87.58% in the treated sample compared to the control sample. The latent heat of decomposition for the 1st and 2nd peak of the treated sample was increased by 12.77% and 5.42% respectively, compared with the control sample. The weight loss was increased by 9.35%; however, the residual weight was significantly reduced by 85.32% in the treated sample compared to the control sample. The maximum thermal degradation temperature of the treated sample was increased by 2.87% compared to the control sample. Hence, the Biofield Energy Treated L-cysteine might show better solubility, dissolution, bioavailability, and be more thermal stability in the pharmaceutical formulations, which would be more efficacious in the treatment of diabetes, cancer, psychosis, and seizures compared to the control sample.

Keyword: L-cysteine; The Trivedi Effect[®]; Energy of consciousness healing treatment; Complementary and alternative medicine; PSA; PXRD; DSC; TGA

Introduction

Cysteine is an essential amino acid that contains sulphur, which allows it to get bonded and maintain its structure within the body [1]. Cysteine is considered an essential as it is the basic building block of the glutathione formation (mother antioxidant) and used by the body to produce taurine, i.e., also an amino acid [2]. L-cysteine had several other uses that help in improving the overall health status of humans. One of its supplements, N-acetyl-L-cysteine (NAC), is used for improving the level of glutathione within the body, as the right glutathione level supports the functioning of brain, lungs, and immunity, and helps in liver detoxification [3]. L-cysteine also acts as a scavenger that fights with the free radicals of the body. Such radicals cause cellular damage in the body by the process of oxidative stress; therefore, L-cysteine preserves the glutathione in the body and improves the antioxidant capacity [4,5]. The supplements containing L-cysteine are also used to improve the immunity in postmenopausal women; prevent the side effects from toxic chemicals and drug reactions; treat

infertility in men having the poor quality of semen; improve the digestive capacity; slow the aging process [6-9]. Other functions of L-cysteine in the body includes balancing the blood sugar levels, relieving the symptoms of bronchitis or chronic obstructive pulmonary disease (COPD), and treating some psychiatric disorders [10-12]. The physicochemical properties of amino acids, such as L-cysteine, play important role in its biological performance within the body. Thus, efforts were made by several researchers to improve such physicochemical profile of the compound that ultimately affects their biological activities, such as improving the solubility and absorption by reducing the particle size, increasing the surface area, or modifying the crystal morphology [13,14]. In this scenario, the Biofield Energy Treatment is known for its significant impact on various properties of living and non-living objects [15,16].

The Biofield energy is a unique phenomenon that involves the traditional as well as the contemporary models of energy medicine and is used as the Complementary and Alternative

Medicine (CAM) to fight against various diseases and disorders [17-19]. The Biofield Energy Healing is an Energy therapy that is used in wide population of the USA and also accepted by the National Centre for Complementary and Alternative Medicine (NCCAM) along with Ayurvedic medicine, traditional Chinese herbs and medicines, naturopathy, essential oils, homeopathy, yoga, meditation, massage, acupuncture, acupressure, Tai Chi, Qi Gong, deep breathing, special diets, relaxation techniques, aromatherapy, guided imagery, healing touch, Reiki, chiropractic/osteopathic manipulation, movement therapy, hypnotherapy, pilates, Rolfing structural integration, mindfulness, cranial sacral therapy, and applied prayer [20]. Thus, an expert human can harness energy from the universal and can transmit it to any living organism(s) or non-living object(s) around the globe. Similarly, the Trivedi Effect®-Consciousness Energy Healing Treatment has shown remarkable impacts in the field of agriculture science [21,22], microbiology [23-25], metals and ceramics [26,27], livestock [28], biotechnology [29,30], and human health and wellness [31-33]. Moreover, the impact of The Biofield Energy Treatment is also evident on the physicochemical and thermal properties of various organic and pharmaceutical compounds [34-36]. Thus, this study was done with the objective to determine the effect of the Biofield Energy Healing Treatment (the Trivedi Effect®) on the physicochemical and thermal properties of L-cysteine with the help of several analytical techniques such as particle size analysis (PSA), powder X-ray diffraction (PXRD), differential scanning calorimetry (DSC), and thermogravimetric analysis (TGA)/differential thermogravimetric analysis (DTG).

Thus, this study was also aimed to analyse the impact of the Biofield Energy Healing Treatment (The Trivedi Effect®) on the physicochemical and thermal properties of ascorbic acid by using various analytical techniques such as, particle size analysis (PSA), powder X-ray diffraction (PXRD), thermogravimetric analysis (TGA)/ differential thermogravimetric analysis (DTG), and differential scanning calorimetry (DSC).

Materials and Methods

Chemicals and reagents

L-cysteine was purchased from Alfa Aesar, USA. All other chemicals used during the experiments were of analytical grade available in India.

Consciousness energy healing treatment strategies

In this study, the test compound used was L-cysteine, which was divided into two parts, i.e., control and treated. The control sample was not given the Biofield Energy Treatment; however, the treated part of L-cysteine received the Energy of Consciousness Healing Treatment by the renowned Biofield Energy Healer, Gopal Nayak (India), and considered as the Biofield Energy Treated sample. The process of Biofield Energy Treatment involves keeping the sample under the standard laboratory conditions and then the Biofield Energy Healer

provided the Trivedi Effect®-Energy of Consciousness Healing Treatment to the sample, remotely, for 3 minutes through the Unique Energy Transmission process. The control L-cysteine was further subjected to a “sham” healer under the similar laboratory conditions, who did not have any knowledge about the Biofield Energy Healing Treatment. The control and the Biofield Energy Treated L-cysteine samples were kept in similar sealed conditions and further characterized by using PSA, PXRD, DSC, and TGA/DTG techniques.

Characterization

Particle size analysis (PSA): The particle size analysis of the L-cysteine was conducted on Malvern Mastersizer 2000, from the UK with a detection range between 0.01 μm to 3000 μm using wet method [37,38]. The sample unit (Hydro MV) was filled with a dispersant medium (sunflower oil), and the stirrer operated at 2500rpm. PSA of L-cysteine was performed to obtain the average particle size distribution. Where d (0.1) μm, d (0.5) μm, d (0.9) μm represent particle diameter corresponding to 10%, 50%, and 90% of the cumulative distribution. D (4,3) represents the average mass-volume diameter, and SSA is the specific surface area (m²/g). The calculations were done by using software Mastersizer Ver. 5.54.

The percent change in particle size (d) for at below 10% level (d₁₀), 50% level (d₅₀), 90% level (d₉₀), and D (4,3) was calculated using the following equation 1:

$$\% \text{ change in particle size} = \frac{[d_{\text{Treated}} - d_{\text{Control}}]}{d_{\text{Control}}} \times 100 \quad (1)$$

Where d_{control} and d_{Treated} are the particle sizes (μm) at below 10% level (d₁₀), 50% level (d₅₀), and 90% level (d₉₀) of the control and the Biofield Energy Treated samples, respectively. The percent change in surface area (S) was calculated using the following equation 2:

$$\% \text{ change in surface area} = \frac{[S_{\text{Treated}} - S_{\text{Control}}]}{S_{\text{Control}}} \times 100 \quad (2)$$

Where S_{control} and S_{Treated} are the surface area of the control and the Biofield Energy Treated L-cysteine, respectively.

Powder X-ray Diffraction (PXRD) Analysis: The PXRD analysis of L-cysteine was performed with the help of RigakuMiniFlex-II Desktop X-ray diffractometer (Japan) [39,40]. The Cu Kα radiation source tube output voltage used was 30 kV and tube output current was 15 mA. Scans were performed at room temperature. The average size of individual crystallites was calculated from XRD data using the Scherrer's formula (3):

$$G = \frac{k\lambda}{\beta \cos \theta} \quad (3)$$

Where k is the equipment constant (0.94), G is the crystallite size in nm, λ is the radiation wavelength (0.154056 nm for Kα1 emission), β is the full-width at half maximum (FWHM), and θ is the Bragg angle [41]. The percent change in crystallite size (G) of L-cysteine was calculated using the following equation 4:

$$\% \text{ change in crystallite size} = \frac{[G_{\text{Treated}} - G_{\text{Control}}]}{G_{\text{Control}}} \times 100 \quad (4)$$

Where G_{control} and G_{Treated} are the crystallite size of the control and the Biofield Energy Treated samples, respectively.

Differential Scanning Calorimetry (DSC): The DSC analysis of L-cysteine was performed with the help of DSC Q200, TA instruments. Sample of 1-5 mg was loaded to the aluminium sample pan at a heating rate of 10°C/min from 30°C to 350°C [37, 38]. The % change in melting point (T) was calculated using the following equation 5:

$$\% \text{ change in melting point} = \frac{[T_{\text{Treated}} - T_{\text{Control}}]}{T_{\text{Control}}} \times 100 \quad (5)$$

Where T_{control} and T_{Treated} are the melting point of the control and treated samples, respectively.

The percent change in the latent heat of fusion (ΔH) was calculated using the following equation 6:

$$\% \text{ change in latent heat of fusion} = \frac{[\Delta H_{\text{Treated}} - \Delta H_{\text{Control}}]}{\Delta H_{\text{Control}}} \times 100 \quad (6)$$

Where $\Delta H_{\text{control}}$ and $\Delta H_{\text{Treated}}$ are the latent heat of fusion of the control and treated L-cysteine, respectively.

Thermal Gravimetric Analysis (TGA)/ Differential Thermogravimetric Analysis (DTG): TGA/DTG thermograms of L-cysteine were obtained with the help of TGA Q50 TA

instruments. A sample of 5 mg was loaded to the platinum crucible at a heating rate of 10°C/min from 25°C to 1000°C with the recent literature [37, 38]. The % change in weight loss (W) was calculated using the following equation 7:

$$\% \text{ change in weight loss} = \frac{[W_{\text{Treated}} - W_{\text{Control}}]}{W_{\text{Control}}} \times 100 \quad (7)$$

Where W_{control} and W_{Treated} are the weight loss of the control and the Biofield Energy Treated L-cysteine, respectively. The % change in maximum thermal degradation temperature (T_{max}) (M) was calculated using the following equation 8:

$$\% \text{ change in Tmax (M)} = \frac{[M_{\text{Treated}} - M_{\text{Control}}]}{M_{\text{Control}}} \times 100 \quad (8)$$

Where M_{control} and M_{Treated} are the T_{max} values of the control and the Biofield Energy Treated L-cysteine, respectively.

Results and Discussion

Particle size analysis (PSA)

The particle size analysis of the control and the Biofield Energy Treated L-cysteine samples corresponding to d_{10} , d_{50} , d_{90} , and D (4, 3) was done (Table 1) to determine the impact of the Biofield Energy Treatment on the particle size distribution of L-cysteine. It revealed that the particle size distribution of the Biofield Energy Treated sample at d_{10} , d_{50} , d_{90} , and D (4, 3) was significantly reduced by 11.96%, 9.01%, 4.92%, and 7.66%, respectively compared to the control sample.

Table 1: Particle size distribution of the control and the Biofield Energy Treated L-cysteine.

Parameter	d_{10} (μm)	d_{50} (μm)	d_{90} (μm)	D (4,3) (μm)	SSA(m^2/g)
Control	263.64	465.93	806.63	504.52	0.014
Biofield Treated	232.1	423.97	766.95	465.87	0.016
Percent change* (%)	-11.96	-9.01	-4.92	-7.66	14.28

d_{10} , d_{50} , and d_{90} : particle diameter corresponding to 10%, 50%, and 90% of the cumulative distribution, D (4,3): the average mass-volume diameter, and SSA: the specific surface area. *denotes the percentage change in the Particle size distribution of the Biofield Energy Treated sample with respect to the control sample.

Such reduction in the particle sizes of the Biofield Energy Treated sample after the Biofield Energy Treatment resulted in 14.28% increase in the specific surface area of the Biofield Energy Treated sample (0.016 m^2/g), in comparison to the untreated L-cysteine sample (0.014 m^2/g). Several types of research were conducted nowadays that correlate the particle size and surface area of the compound with its solubility and dissolution profile [42,43]. Moreover, the reduced particle size and increased surface area of the compound are known for improving the solubility, absorption, and bioavailability performance in the body [44]. Thus, it is assumed that the Biofield Energy Treated L-cysteine might show better solubility and dissolution rate within the body that ultimately enhances its bioavailability in comparison to the untreated sample.

Powder X-ray diffraction (PXRD) analysis

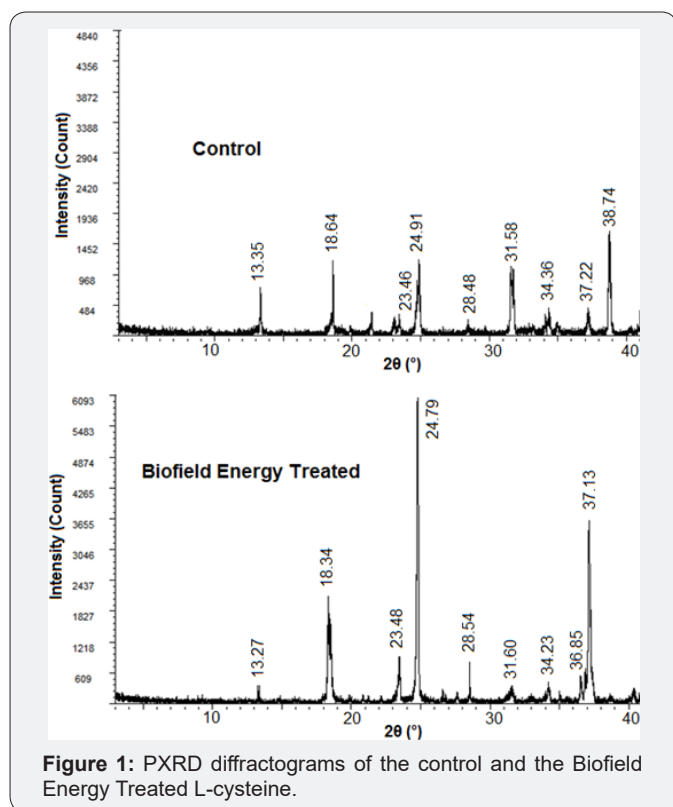
Figure 1 shows the diffractograms of the control and the Biofield Energy Treated L-cysteine samples; and both contains sharp and intense peaks, thereby indicating their crystalline nature. The analysis regarding the changes in the

peak intensities and the crystallite sizes of the Biofield Energy Treated sample in comparison to the control sample was done and presented in Table 2. The analysis of the diffractograms revealed alterations in the Bragg's angle of the characteristic peaks of the Biofield Energy Treated sample as compared to the control sample. Also, the highest peak intensity (100%) was observed at 2θ equal to 37.13° in the control sample; while in the Biofield Energy Treated sample at 2θ equal to 24.91° . The significant alterations were observed in the peak intensities and the crystallite sizes of the Biofield Energy Treated L-cysteine sample as compared to the control sample. The Biofield Energy Treated sample showed changes in the peak intensities ranging from -86.73% to 456.65%; while the crystallite sizes were altered ranging from -74.91% to 451.22%, compared to the control sample. Such changes corresponding to the characteristic diffraction peaks of the Biofield Energy Treated sample showed that the crystallinity and crystalline structure of L-cysteine sample might get altered after the Biofield Energy Treatment as compared to the untreated sample.

Table 2: PXRD data for the control and the Biofield Energy Treated L-cysteine.

Entry No.	Bragg angle (°2θ)		Intensity (cps)			Crystallite size (G, nm)		
	Control	Treated	Control	Treated	% change a	Control	Treated	% change b
1	13.35	13.27	55	7.3	-86.73	943	5198	451.22
2	18.64	18.34	71	198	178.87	857	711	-17.04
3	23.46	23.48	20.3	113	456.65	626	532	-15.02
4	24.91	24.79	176	664	277.27	352	764	117.05
5	28.48	28.54	12.9	20.4	58.14	590	1467	148.64
6	31.58	31.6	106	51.6	-51.32	817	205	-74.91
7	34.36	34.23	31	44	41.94	627	734	17.07
8	37.22	36.85	41	63	53.66	506	927	83.2
9	38.74	37.13	185	448	142.16	690	732	6.09

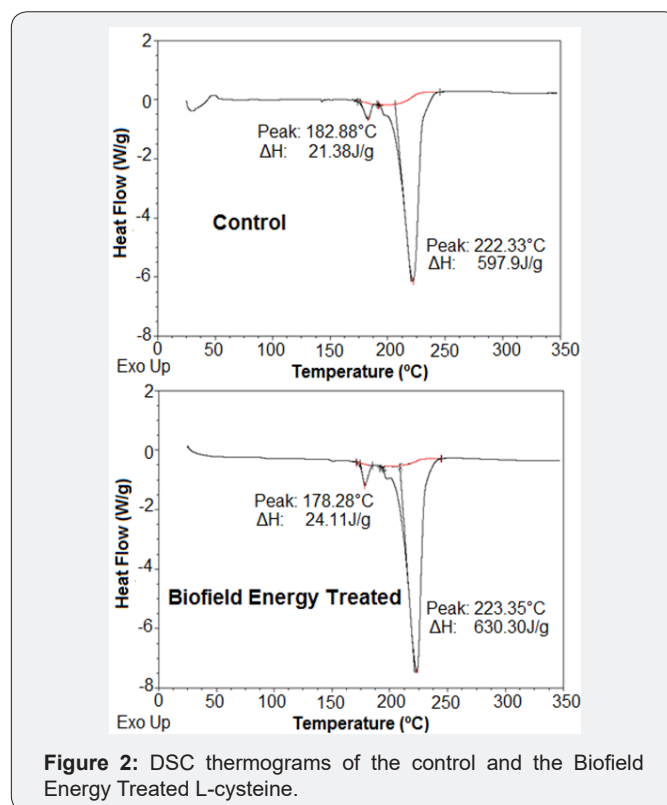
^adenotes the percentage change in the peak intensity of the Biofield Energy Treated sample with respect to the control sample; ^bdenotes the percentage change in the crystallite size of the Biofield Energy Treated sample with respect to the control sample.



The average crystallite size of the Biofield Energy Treated sample was 1252.22 nm, which was increased by 87.58% compared to the control sample (667.56 nm). The significant alterations in the crystal morphology and the crystallinity of the compounds after the Biofield Energy Treatment were reported previously in various studies. They reported the occurrence of such changes based on the alterations in their peak intensities and crystallite sizes of the Biofield Energy Treated compounds that might indicate the formation of a novel polymorph of the compound [45,46]. Thus, the Biofield Energy Treated L-cysteine showed significant changes in the peak intensities and crystallite size corresponding to the characteristic peaks that might take place as a result of the new

polymorph formation of L-cysteine. The literature reported the improved bioavailability profile of drug as a result of the physical modifications, i.e., alteration in the crystal habit of the drug [47]. Hence, the Biofield Energy Treated L-cysteine might show improved bioavailability as compared to the untreated sample.

Differential scanning calorimetry (DSC) analysis



The DSC thermograms of the control and the Biofield Energy Treated sample are shown in Figure 2, that are further analysed to determine the melting and other thermal behaviours of both the sample [48]. The literature reported that L-cysteine got decomposed instead of sublimation during its thermal

heating. It was mentioned that the peak in DSC thermogram was present at the same temperature as the drop in the TGA thermogram. Thus, the DSC peak temperature coincides with the TGA drop thereby, indicated the process of decomposition in place of melting during the heating of L-cysteine [48,49].

There were two peaks present in the thermograms of the control and the Biofield Energy Treated sample. The results

revealed the alterations in the decomposition temperature of the 1st and 2nd peak of the Biofield Energy Treated sample by -2.51% and 0.46%, respectively in compared to the control sample. The latent heat of decomposition ($\Delta H_{decomposition}$) for 1st and 2nd peak of the Biofield Energy Treated L-cysteine sample was significantly increased by 12.77% and 5.42%, respectively, compared to the control sample (Table 3).

Table 3: Comparison of DSC data between the control and the Biofield Energy Treated L-cysteine.

Peak	Description	Melting Point (°C)	$\Delta H_{decomposition}$ (J/g)
Peak 1	Control sample	182.88	21.38
	Biofield Treated sample	178.28	24.11
	% Change*	-2.51	12.77
Peak 2	Control sample	222.33	597.9
	Biofield Treated sample	223.35	630.3
	% Change*	0.46	5.42

ΔH : Latent heat of decomposition; *denotes the percentage change of the Biofield Energy Treated sample with respect to the control sample.

The results indicated that the Biofield Energy Treated sample started decomposing 4.6° earlier temperature as compared to the control sample, which might be due to some changes in the particle size and crystallization structure of the L-cysteine [48,50] after the Biofield Energy Treatment. Thus, the Biofield Energy Treated sample showed an increase in thermal degradation in comparison to the untreated L-cysteine sample.

Thermal gravimetric analysis (TGA)/ Differential thermogravimetric analysis (DTG)

The weight loss of the L-cysteine samples during the thermal degradation was analysed from the TGA thermograms (Figure 3) of the control and the Biofield Energy Treated sample. Also, the degradation profile of both the samples were observed like the reported literature [49]. The analysis of both the thermograms showed that the total weight loss of the control sample was 90.12%; whereas it was observed as 98.55% for the Biofield Energy Treated L-cysteine sample. Thus, the total weight loss during the thermal degradation of the Biofield Energy Treated sample was increased significantly by 9.35% that resulted in 85.32% decrease in the residual mass compared with the control sample (Table 4). Hence, the thermal degradation of the Biofield Energy Treated sample was increased after the Biofield Energy Treatment in comparison to the untreated sample.

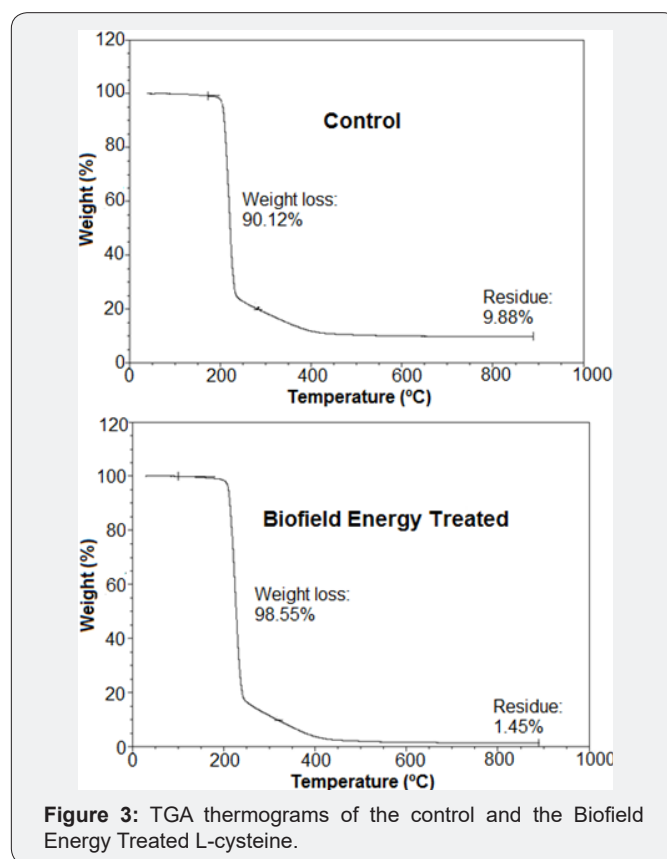


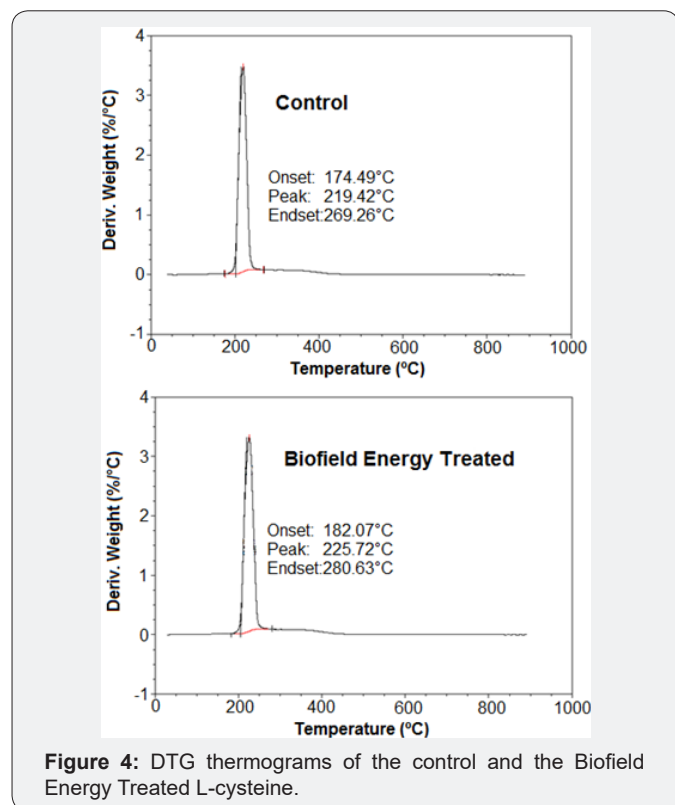
Figure 3: TGA thermograms of the control and the Biofield Energy Treated L-cysteine.

Table 4: TGA/DTG data of the control and the Biofield Energy Treated samples of L-cysteine.

Sample	TGA		DTG
	Total weight loss (%)	Residue %	T _{max} (°C)
Control	90.12	9.88	219.42
Biofield Energy Treated	98.55	1.45	225.72
% Change*	9.35	-85.32	2.87

*denotes the percentage change of the Biofield Energy Treated sample with respect to the control sample,
T_{max} = the temperature at which maximum weight loss takes place in TG or peak temperature in DTG.

The DTG data (Table 4) (Figure 4) of the Biofield Energy Treated sample showed the maximum thermal degradation temperature (T_{max}) at 225.72 °C, which was improved by ~ 6 °C (2.87%) as compared to the T_{max} of the control sample (219.42 °C). Hence, the overall TGA/DTG studies revealed that the thermal stability profile of the Biofield Energy Treated L-cysteine sample was altered after the Biofield Energy Treatment as compared with the untreated sample.



Conclusion

The study results suggested that there was a significant impact of the Trivedi Effect®-Consciousness Energy Healing Treatment on various properties of the Biofield Energy Treated L-cysteine sample related to their physicochemical and thermal profile. The PSD data showed that the particle size values of the Biofield Energy Treated sample were significantly reduced at d_{10} , d_{50} , d_{90} , and $D(4, 3)$ by 11.96%, 9.01%, 4.92%, and 7.66%, respectively, compared to the untreated sample. The specific surface area of the Biofield Energy Treated L-cysteine was significantly increased by 14.28% in comparison to the untreated L-cysteine. The PXRD peak intensities of the Biofield Energy Treated L-cysteine were observed to be changed ranging from -86.73% to 456.65% and crystallite sizes showed alterations ranging from -74.91% to 451.22% as compared to the control sample. The average crystallite size of the Biofield Energy Treated sample was significantly increased by 87.58%, as compared to the control L-cysteine sample. The DSC thermograms of the control and the Biofield Energy Treated sample showed two peaks in their thermograms that

are related to the decomposition of L-cysteine sample during heating. However, the corresponding to 1st and 2nd peak were also observed to be significantly increased by 12.77% and 5.42%, respectively, compared to the control L-cysteine sample. The TGA/DTG data indicating that the Biofield Energy Treated sample showed 9.35% increase in total weight loss of the L-cysteine sample that causes a significant 85.32% reduction in the residue amount compared to the untreated sample. However, the of the Biofield Energy Treated sample was increased by 2.87% compared to the control sample. Thus, the overall data showed the reduced particle sizes and increased surface area of the Biofield Energy Treated sample with alterations in the crystal structure, which might increase the solubility, absorption, and bioavailability of L-cysteine within the body. Also, the results indicating significant changes in the thermal degradation and stability profile of the Biofield Energy Treated L-cysteine sample compared to the untreated sample. Therefore, the Trivedi Effect®-Consciousness Energy Healing Treated L-cysteine might improve the properties that might ensure its better performance and therapeutic response against various diseases, i.e., diabetes, cancer, psychosis, and seizures.

Acknowledgement

The authors are grateful to Central Leather Research Institute, SIPRA Lab. Ltd., Trivedi Science, Trivedi Global, Inc., Trivedi Testimonials, and Trivedi Master Wellness for their assistance and support during this work.

References

1. Brosnan JT, Brosnan ME (2006) The sulfur-containing amino acids: an overview. *J Nutr*, 136: 1636S-1640S.
2. Ripps H, Shen W (2012) Review: Taurine: A "very essential" amino acid. *Mol Vis*, 18: 2673-2686.
3. Kerksick C, Willoughby D (2005) The Antioxidant Role of Glutathione and N-Acetyl-Cysteine Supplements and Exercise-Induced Oxidative Stress. *J Int Soc Sports Nutr*; 2: 38-44.
4. Lobo V, Patil A, Phatak A, Chandra N (2010) Free radicals, antioxidants and functional foods: Impact on human health. *Pharmacogn Rev* 4: 118-126.
5. Quig D (1998) Cysteine metabolism and metal toxicity. *Altern Med Rev* 3: 262-270.
6. Arranz L, Fernández C, Rodríguez A, Ribera JM, De la Fuente M (2008) The glutathione precursor N-acetylcysteine improves immune function in postmenopausal women. *Free Radic Biol Med* 45: 1252-1262.
7. McClure EA, Gipson CD, Malcolm RJ, Kalivas PW, Gray KM (2014) Potential Role of N-Acetylcysteine in the Management of Substance Use Disorders. *CNS Drugs*, 28: 95-106.
8. Barekat F, Tavalae M, Deemeh MR, Bahreinian M, Azadi L, et al. (2016) A Preliminary Study: N-acetyl-L-cysteine Improves Semen Quality following Varicocele. *Int J Fertil Steril* 10: 120-126.
9. Guijarro LG, Mate J, Gisbert JP, Perez-Calle JL, Marin-Jimenez I, et al. (2008) N-acetyl-L-cysteine combined with mesalamine in the treatment of ulcerative colitis: Randomized, placebo-controlled pilot study. *World J Gastroenterol* 14: 2851-2857.

10. Jain SK, Velusamy T, Croad JL, Rains JL, Bull R (2009) L-cysteine supplementation lowers blood glucose, glycated hemoglobin, CRP, MCP-1, oxidative stress and inhibits NFkB activation in the livers of Zucker diabetic rats. *Free Radic Biol Med* 46: 1633-1638.
11. Dekhuijzen P, van Beurden W (2006) The role for N-acetylcysteine in the management of COPD. *Int J Chron Obstruct Pulmon Dis* 1: 99-106.
12. Dean O, Giorlando F, Berk M (2011) N-acetylcysteine in psychiatry: current therapeutic evidence and potential mechanisms of action. *J Psychiatry Neurosci* 36: 78-86.
13. Barlow RB (1974) Physicochemical properties and biological activity: thermodynamic properties of compounds related to acetylcholine assessed from depression of freezing-point and enthalpies of dilution. *Br J Pharmacol*, 51: 413-426.
14. Braakhuis HM, Park MV, Gosens I, De Jong WH, Cassee FR (2014) Physicochemical characteristics of nanomaterials that affect pulmonary inflammation. *Part Fibre Toxicol*, 11: 18.
15. Trivedi MK, Branton A, Trivedi D, Nayak G, Sethi KK, et al. (2016) Isotopic abundance ratio analysis of biofield energy treated indole using gas chromatography-mass spectrometry. *Science Journal of Chemistry* 4: 41-48.
16. Koster DA, Trivedi MK, Branton A, Trivedi D, Nayak G, et al. (2018) Evaluation of biofield energy treated vitamin D₃ on bone health parameters in human bone osteosarcoma cells (MG-63). *Biochemistry and Molecular Biology* 3: 6-14.
17. Guarneri E, King RP (2015) Challenges and Opportunities Faced by Biofield Practitioners in Global Health and Medicine: A White Paper. *Global Advances in Health and Medicine* 4: 89-96.
18. Barnes PM, Bloom B, Nahin RL (2008) Complementary and alternative medicine use among adults and children: United States, 2007. *Natl Health Stat Report* 12: 1-23.
19. Frass M, Strassl RP, Friehs H, Müllner M, Kundi M, et al. (2012) Use and acceptance of complementary and alternative medicine among the general population and medical personnel: A Systematic Review. *Ochsner J* 12: 45-56.
20. Koithan M (2009) Introducing Complementary and Alternative Therapies. *J Nurse Pract* 5: 18-20.
21. Trivedi MK, Branton A, Trivedi D, Nayak G, Mondal SC, et al. (2015) Morphological characterization, quality, yield and DNA fingerprinting of biofield energy treated alphonso mango (*Mangifera indica* L.). *Journal of Food and Nutrition Sciences* 3: 245-250.
22. Trivedi MK, Branton A, Trivedi D, Nayak G, Mondal SC, et al. (2015) Evaluation of biochemical marker - Glutathione and DNA fingerprinting of biofield energy treated *Oryza sativa*. *American Journal of BioScience* 3: 243-248.
23. Trivedi MK, Patil S, Shettigar H, Mondal SC, Jana S (2015) Evaluation of biofield modality on viral load of Hepatitis B and C viruses. *J Antivir Antiretrovir* 7: 083-088.
24. Trivedi MK, Patil S, Shettigar H, Mondal SC, Jana S (2015) An impact of biofield treatment: Antimycobacterial susceptibility potential using BACTEC 460/MGIT-TB System. *Mycobact Dis* 5: 189.
25. Trivedi MK, Branton A, Trivedi D, Nayak G, Charan S, et al. (2015) Phenotyping and 16S rDNA analysis after biofield treatment on *Citrobacter braakii*: A urinary pathogen. *J Clin Med Genom* 3: 129.
26. Trivedi MK, Tallapragada RM, Branton A, Trivedi D, Nayak G, et al. (2015) Analysis of physical, thermal, and structural properties of biofield energy treated molybdenum dioxide. *International Journal of Materials Science and Applications* 4: 354-359.
27. Trivedi MK, Tallapragada RM, Branton A, Trivedi D, Nayak G, et al. (2015) The potential impact of biofield energy treatment on the physical and thermal properties of silver oxide powder. *International Journal of Biomedical Science and Engineering* 3: 62-68.
28. Trivedi MK, Branton A, Trivedi D, Nayak G, Mondal SC, et al. (2015) Effect of Biofield Treated Energized Water on the Growth and Health Status in Chicken (*Gallus gallusdomesticus*). *Poult Fish WildlSci* 3: 140.
29. Nayak G, Altekar N (2015) Effect of biofield treatment on plant growth and adaptation. *J Environ Health Sci* 1: 1-9.
30. Branton A, Jana S (2017) The influence of energy of consciousness healing treatment on low bioavailable resveratrol in male *Sprague Dawley* rats. *International Journal of Clinical and Developmental Anatomy* 3: 9-15.
31. Kinney JP, Trivedi MK, Branton A, Trivedi D, Nayak G, et al. (2017) Overall skin health potential of the biofield energy healing based herbomineral formulation using various skin parameters. *American Journal of Life Sciences* 5: 65-74.
32. Branton A, Jana S (2017) Effect of The biofield energy healing treatment on the pharmacokinetics of 25-hydroxyvitamin D₃ [25(OH) D₃] in rats after a single oral dose of vitamin D₃. *American Journal of Pharmacology and Phytotherapy* 2: 11-18.
33. Singh J, Trivedi MK, Branton A, Trivedi D, Nayak G, et al. (2017) Consciousness energy healing treatment based herbomineral formulation: A safe and effective approach for skin health. *American Journal of Pharmacology and Phytotherapy* 2: 1-10.
34. Trivedi MK, Branton A, Trivedi D, Shettigar H, Bairwa K, et al. (2015) Fourier Transform Infrared and Ultraviolet-Visible Spectroscopic Characterization of Biofield Treated Salicylic Acid and Sparfloxacin. *Nat Prod Chem Res* 3: 186.
35. Trivedi MK, Branton A, Trivedi D, Nayak G, Nykvist CD, et al. (2017) Evaluation of the Trivedi Effect®- Energy of Consciousness Energy Healing Treatment on the physical, spectral, and thermal properties of zinc chloride. *American Journal of Life Sciences*. 5: 11-20.
36. Trivedi MK, Patil S, Shettigar H, Bairwa K, Jana S (2015) Spectroscopic characterization of biofield treated metronidazole and tinidazole. *Med chem* 5: 340-344.
37. Trivedi MK, Sethi KK, Panda P, Jana S (2017) Physicochemical, thermal and spectroscopic characterization of sodium selenate using XRD, PSD, DSC, TGA/DTG, UV-vis, and FT-IR. *Marmara Pharmaceutical Journal* 21/2: 311-318.
38. Trivedi MK, Sethi KK, Panda P, Jana S (2017) A comprehensive physicochemical, thermal, and spectroscopic characterization of zinc (II) chloride using Xray diffraction, particle size distribution, differential scanning calorimetry, thermogravimetric analysis/differential thermogravimetric analysis, ultravioletvisible, and Fourier transforminfrared spectroscopy. *International Journal of Pharmaceutical Investigation* 7: 33-40.
39. Zhang T, Paluch K, Scalabrino G, Frankish N, Healy AM, et al. (2015) Molecular structure studies of (1S,2S)-2-benzyl-2,3-dihydro-2-(1Hinden-2-yl)-1H-inden-1-ol. *J Mol Struct* 1083: 286-299.
40. Desktop X-ray Diffractometer "MiniFlex+". *The Rigaku Journal* 14: 29-36, 1997.
41. Langford JI, Wilson AJC (1978) Scherrer after sixty years: A survey and some new results in the determination of crystallite size. *J ApplCryst* 11: 102-113.
42. Loh ZH, Samanta AK, Heng PWS (2015) Overview of milling techniques for improving the solubility of poorly water-soluble drugs. *Asian J Pharm*, 10: 255-274.
43. Khadka P, Roa J, Kim H, Kim I, Kim JT, et al. (2014) Pharmaceutical particle technologies: An approach to improve drug solubility, dissolution and bioavailability. *Asian J Pharm*, 9: 304-316.

44. Hu J, Johnston KP, Williams RO (2004) Nanoparticle engineering processes for enhancing the dissolution rates of poorly water soluble drugs. *Drug Dev Ind Pharm*, 30: 233-245.
45. Trivedi MK, Branton A, Trivedi D, Nayak G, Lee AC, et al. (2017) Evaluation of the impact of biofield energy healing treatment (the Trivedi Effect®) on the physicochemical, thermal, structural, and behavioural properties of magnesium gluconate. *International Journal of Nutrition and Food Sciences*. 6: 71-82.
46. Trivedi MK, Branton A, Trivedi D, Nayak G, Plikerd WD, et al. (2017) Evaluation of the physicochemical, spectral, thermal and behavioral properties of sodium selenate: influence of the energy of consciousness healing treatment. *American Journal of Quantum Chemistry and Molecular Spectroscopy* 2: 18-27.
47. Savjani KT, Gajjar AK, Savjani JK (2012) Drug Solubility: Importance and Enhancement Techniques. *ISRN Pharmaceutics*, 2012: Article ID 195727.
48. Zhao Z, Xie M, Li Y, Chen A, Li G, et al. (2015) Formation of curcumin nanoparticles *via* solution enhanced dispersion by supercritical CO₂. *Int J Nanomedicine* 10: 3171-3181.
49. Weiss IM, Muth C, Drumm R, Kirchner HOK (2018) Thermal decomposition of the amino acids glycine, cysteine, aspartic acid, asparagine, glutamic acid, glutamine, arginine and histidine. *BMC Biophysics* 11: 2.
50. Sovizi MR, Hajimirsadeghi SS, Naderizadeh B (2009) Effect of particle size on thermal decomposition of nitrocellulose. *J Hazard Mater*, 168: 1134-1139.



This work is licensed under Creative Commons Attribution 4.0 License
DOI: [10.19080/NFSIJ.2018.08.555726](https://doi.org/10.19080/NFSIJ.2018.08.555726)

**Your next submission with Juniper Publishers
will reach you the below assets**

- Quality Editorial service
- Swift Peer Review
- Reprints availability
- E-prints Service
- Manuscript Podcast for convenient understanding
- Global attainment for your research
- Manuscript accessibility in different formats
(Pdf, E-pub, Full Text, Audio)
- Unceasing customer service

Track the below URL for one-step submission
<https://juniperpublishers.com/online-submission.php>